Available online at www.sciencedirect.com
SCIENCE DIRECT®
Biochimica et Biophysica Acta 1612 (2003) 65–75
BIOCHIMICA ET BIOPHYSICA ACTA
BBA
www.bba-direct.com

Single-step immunoaffinity purification and characterization of dodecylmaltoside-solubilized human neutrophil flavocytochrome *b*

Ross M. Taylor, James B. Burritt, Thomas R. Foubert, Meagan A. Snodgrass, Kim C. Stone, Danas Baniulis, Jeannie M. Gripentrog, Connie Lord, Algirdas J. Jesaitis*

Department of Microbiology, Montana State University, 109 Lewis Hall, Bozeman, MT 59717-3520, USA

Received 18 November 2002; received in revised form 3 March 2003; accepted 5 March 2003

Abstract

Flavocytochrome *b* (Cyt *b*) is a heterodimeric, integral membrane protein that serves as the central component of an electron transferase system employed by phagocytes for elimination of bacterial and fungal pathogens. This report describes a rapid and efficient single-step purification of Cyt *b* from human neutrophil plasma membranes by solubilization in the nonionic detergent dodecylmaltoside (DDM) and immunoaffinity chromatography. A similar procedure for isolation of Cyt *b* directly from intact neutrophils by a combination of heparin and immunoaffinity chromatography is also presented. The stability of Cyt *b* was enhanced in DDM relative to previously employed solubilizing agents as determined by both monitoring the heme spectrum in crude membrane extracts and assaying resistance to proteolytic degradation following purification. Gel filtration chromatography and dynamic light scattering indicated that DDM maintains a predominantly monodisperse population of Cyt *b* following immunoaffinity purification. The high degree of purity obtained with this isolation procedure allowed for direct determination of a 2:1 heme to protein stoichiometry, confirming previous structural models. Analysis of the isolated heterodimer by matrix-assisted laser desorption/ionization (MALDI) mass spectrometry allowed for accurate mass determination of $p22^{phox}$ as indicated by the gene sequence. Affinity-purified Cyt *b* was functionally reconstituted into artificial bilayers and demonstrated that catalytic activity of the protein was efficiently retained throughout the purification procedure.

Keywords: Flavocytochrome *b*; Immunoaffinity; Purification; Heme; Dodecylmaltoside

1. Introduction

Neutrophils and other phagocytes play an integral role in innate immunity by serving as a first line of defense against invading bacterial and fungal pathogens. Following activation, neutrophils migrate from the blood to sites of infection and eliminate infectious agents by a combination of phagocytosis and exposure to a wide array of toxic proteins, hydrolytic enzymes, and reactive oxygen species [1]. The generation of reactive oxygen species has been demonstrated an indispensable component of the neutrophils' microbicidal capability. Superoxide generation by the phagocyte nicotinamide adenine dinucleotide (NADPH) oxidase complex initiates this process by catalyzing the transfer of metabolic electrons across the plasma membrane for reduction of molecular oxygen [1]. The importance of NADPH oxidase function is illustrated by individuals deficient in this enzymatic activity who suffer from a condition known as Chronic Granulomatous Disease. This disease state is characterized by recurrent, life-threatening bacterial and fungal infections [2] and the formation of characteristic granuloma in such patients. Consequences of excessive or otherwise inappropriate superoxide production by this complex include a variety of inflammatory disease states [3] and an increased risk of oncogenesis [4].

Abbreviations: AC-PQVRPI-$CONH_2$, the peptide Pro-Gln-Val-Arg-Pro-Ile acetylated at the N-terminus and amidated at the C-terminus; BSA, bovine serum albumin; CMC, critical micelle concentration; Cyt *b*, flavocytochrome *b*; DDM, dodecylmaltoside; DTT, dithiothreitol; EDTA, ethylenediaminetetraacetic acid; FAD, flavin adenine dinucleotide; fMLF, the peptide Met-Leu-Phe formylated at the N-terminus; HEPES, *N*-[2-Hydroxyethyl]piperazine-*N*′-[2-ethanesulfonic acid]; HPLC, high-performance liquid chromatography; LDS, lithium dodecyl sulfate; mAb, monoclonal antibody; MALDI, matrix-assisted laser desorption/ionization; NADPH, nicotinamide adenine dinucleotide; OG, octylglucoside; PMSF, phenylmethylsulfonylfluoride; SDS-PAGE, sodium dodecylsulfate polyacylamide gel electrophoresis; TFA, trifluoroacetic acid; TX-100, Triton X-100

* Corresponding author. Tel.: +1-406-994-4811; fax: +1-406-994-4926.
E-mail address: umbaj@gemini.oscs.montana.edu (A.J. Jesaitis).

0005-2736/03/$ - see front matter © 2003 Elsevier Science B.V. All rights reserved.
doi:10.1016/S0005-2736(03)00086-5

The NADPH oxidase system is composed of both a core electron transferase (flavocytochrome *b*, Cyt *b*) located in the neutrophil plasma membrane and cytosolic, regulatory proteins ($p47^{phox}$, $p67^{phox}$, $p40^{phox}$ and the small G-protein Rac) that translocate to the membrane upon neutrophil activation to initiate superoxide production [1]. Cyt *b* is a heterodimeric, integral membrane protein composed of a 21-kDa subunit ($p22^{phox}$) and a heavily glycosylated, 65-kDa subunit ($gp91^{phox}$; 1). Hydropathy analysis by a number of available predictive algorithms indicates six to eight distinct stretches of primary sequence of sufficient length and hydrophobicity to span the membrane as independent α-helices in the N-terminal domain of $gp91^{phox}$, while similar analysis of $p22^{phox}$ delineates two to three possible membrane spanning helices [5] (D. Banilius, A.J. Jesaitis, unpublished data). Previous studies employing potentiometric titration analysis [6], ESR spectroscopy [7], sequence analysis [5] and chemical modification [8] have suggested two bis-histidine coordinated heme groups in the cytochrome heterodimer. The heme prosthetic groups have been experimentally determined to reside within the membrane-embedded portion of the molecule [9]. Electron transfer from metabolic NADPH to the heme prosthetic groups is mediated by the cytosolic, C-terminal domain of $gp91^{phox}$, which contains consensus sequences found in NADPH and flavin adenine dinucleotide (FAD) binding sites of other redox enzymes [10]. In vitro activity assays have indicated the core, integral membrane component of the NADPH oxidase complex to contain all of the structural elements required for the transfer of electrons from NADPH to molecular oxygen [11]. Although models have been proposed describing the structure and function of Cyt *b*, fundamental questions remain concerning the nature of this enzyme complex. Problems associated with the isolation of sufficient quantities of this low abundance, integral membrane protein have limited the amount of direct biochemical analysis of Cyt *b* and hindered the refinement of current structural models.

The present study describes rapid and efficient methods for immunoaffinity purification human neutrophil Cyt *b* from both intact cells and isolated plasma membrane fractions. Following purification, biochemical and biophysical methods were employed to provide a detailed characterization of the isolated protein–detergent complex.

2. Materials and methods

2.1. Materials

Dodecylmaltoside (DDM) was purchased from Fluka; octylglucoside (OG), phenylmethylsulfonylfluoride (PMSF) and dithiothreitol (DTT) from Calbiochem and Staphylococcal V8 protease obtained from Boehringer Mannheim. FAD, NADPH, superoxide dismutase (SOD), L-α-phosphatidylcholine (type II-S and type IV-S), heparin-Agarose, lithium dodecyl sulfate (LDS), BSA, pyridine, horse heart cytochrome *c*, chymostatin, the mammalian protease inhibitor cocktail (P8340) and Triton X-100 (TX-100) were obtained from Sigma. The Superdex 200 gel filtration column and protein A–Sepharose beads were from Pharmacia; Centricon-50 concentrators from Millipore; SM-2 BioBeads and gel filtration chromatography standards from BioRad; and 3370 96-well microtiter plates from Costar. ProSieve color molecular weight markers were purchased from BMA; α-cyano-4-hydroxycinnamic acid from Aldrich; and nitrocellulose (0.45 μm pore size) from Schleicher & Schuell. High-performance liquid chromatography (HPLC) grade acetonitrile was from Fisher and trifluoroacetic acid (TFA) from Pierce. The elution peptide AC-PQVRPI-$CONH_2$ (AC-, acetylation at the N-terminus of the elution peptide; -$CONH_2$, amidation at the C-terminus of the elution peptide) was obtained from Macromolecular Resources.

Following sodium dodecylsulfate polyacylamide gel electrophoresis (SDS-PAGE), densitometric quantitation was performed using an HP ScanJet II cx scanner and the programs ImageQuant (Software version 3.3, Molecular Dynamics) and Multi-Analyst (Software version 1.1, BioRad laboratories). The activity of reconstituted Cyt *b* was measured on a Molecular Devices SpectraMAX 250 plate reader and data evaluated with SOFTmax Pro software. Absorption measurements were performed on an Agilent absorption spectrophotometer with quartz micro cuvettes obtained from the same supplier. Sonication was conducted with a model 50 Sonic dismembrator probe sonicator obtained from Fisher Scientific. Gel filtration chromatography was conducted on a Hitachi, LS-6200 HPLC with an F-1050 fluorescence detector connected in series with an L-7450A UV–Visible Diode Array Detector. Mass spectra were collected on a Bruker Biflex III time-of-flight matrix-assisted laser desorption/ionization (MALDI) mass spectrometer with instrument configuration modulated in the XACQ software and data analysis conducted in the XMASS software.

2.2. Construction of the 44.1 affinity matrix

Monoclonal antibody (mAb) 44.1 [12] hybridoma culture supernatants were used for construction of the affinity matrix. The 44.1 affinity matrix employed for Cyt *b* purification was constructed by washing 1.25 ml of packed protein A–Sepharose beads three times with PBS and then rotating the beads with 125 ml of hybridoma culture supernatant overnight at 4 °C. The hydridoma supernatant was then removed and the beads washed three times with PBS at room temperature, followed by an additional wash with 10 mM *N*-[2-Hydroxyethyl]piperazine-*N*′-[2-ethanesulfonic acid] (HEPES)/10 mM NaCl/100 mM KCl/1 mM ethylenediaminetetraacetic acid (EDTA), pH-7.4 (Buffer A). For column equilibration, the beads were washed with Buffer A/0.1% DDM at room temperature and then washed one final time by incubation with Buffer A/0.1% DDM for 15 min at 37 °C.

2.3. Cyt b purification from plasma membrane fractions

Neutrophil plasma membranes were prepared as previously described [13] and stored at −70 °C prior to cytochrome purification. For large-scale purifications, 20 ml of thawed neutrophil membranes (~ 1×10^{10} cell equivalents) were washed with 1 M NaCl and centrifuged at 114,000 × *g* for 30 min at 4 °C. Membrane pellets were resuspended by homogenization in 19 ml of Buffer A/0.1 mM DTT/10 μg/ml chymostatin/1 mM PMSF/1 μl/ml P8340. Following addition of DDM to 0.75% from a 20% stock solution, extracts were sonicated briefly and allowed to incubate, with stirring, at room temperature for 1 h. Membrane extracts were then centrifuged at 114,000 × *g* for 30 min at 22 °C and supernatant fractions collected for subsequent purification.

For purification of Cyt *b*, the above DDM membrane extract (20 ml) was tumbled with 1.25 ml of the affinity matrix for 2 h at room temperature. The affinity matrix was subsequently washed three times (10 min per wash) at room temperature with 2 ml of Buffer A/0.5% DDM. Elution of Cyt *b* was achieved by three separate incubations (10 min per incubation) at 37 °C with 2 ml of Buffer A/0.25% DDM containing 1 mM elution peptide AC-PQVRPI-$CONH_2$ (AC-, acetylation at the N-terminus of the elution peptide; -$CONH_2$, amidation at the C-terminus of the elution peptide). Three separate elutions were collected and analyzed for Cyt *b* by absorption spectroscopy.

For removal of elution peptide, Cyt *b*-containing fractions were concentrated to approximately 1 ml in a Centricon-50 concentrator and then dialyzed (with one change of buffer) against 1000 volumes of 50 mM K_2HPO_4/150 mM NaCl/1 mM EGTA/1 mM $MgCl_2$, pH 7.3 overnight at 4 °C. Alternatively, affinity-purified Cyt *b* was concentrated to approximately 0.5 ml and chromatographed at 4 °C on a Superdex 200 gel filtration column at 0.4 ml/min in 50 mM K_2HPO_4/150 mM NaCl/1 mM EGTA/1 mM $MgCl_2$/0.2% DDM, pH-7.3. Cytochrome eluting from the gel filtration column was detected by monitoring the oxidized heme Soret band. The molecular weight of the Cyt *b* protein–detergent complex was estimated by comparison to a calibration curve derived from the migration of gel filtration standards on the Superdex column.

2.4. Cyt b purification from intact neutrophils

Intact neutrophil cells (~ 4.5×10^9 cells) were isolated from whole human blood as previously described [13]. Cells were washed twice with 10 ml of Buffer A and then resuspended in 18 ml of Buffer A/0.1 mM DTT/10 μg/ml chymostatin/1 mM PMSF/1 μl/ml P8340. Following addition of DDM to 1% from a 20% stock solution, the mixture was sonicated briefly and allowed to incubate, with stirring, at 4 °C for 45 min. Whole cell extracts were then centrifuged at 114,000 × *g* for 30 min at 4 °C and supernatant fractions collected for subsequent purification. Supernatant fractions were diluted 2.5-fold in 10 mM HEPES/0.1 mM DTT/10 μg/ml chymostatin/1 mM PMSF/1 μl/ml P8340 and loaded on a 1.5 ml heparin-Agarose column (0.75 ml/min at 4 °C) that had been previously equilibrated in 10 mM HEPES/0.1% DDM. The column was then washed with 10 ml of 10 mM HEPES/0.1% DDM and bound Cyt *b* eluted with Buffer A/0.1 mM DTT/10 μg/ml chymostatin/1 mM PMSF/1 μl/ml P8340/0.1% DDM/900 mM NaCl. Cyt *b* containing fractions eluted from the heparin column were pooled (~ 2.25 ml total) and diluted to 20 ml with Buffer A/0.1 mM DTT/10 μg/ml chymostatin/1 mM PMSF/1 μl/ml P8340/0.1% DDM. Cyt *b* was then purified from this 20 ml fraction by 44.1 affinity purification as previously described.

2.5. Stability analysis

For stability analysis, 3 ml of neutrophil plasma membranes were washed with 1 M NaCl and centrifuged at 114,000 × *g* for 30 min at 4 °C. Membrane pellets were resuspended by homogenization and brief sonication in 3 ml of Buffer A. Resuspended, salt-washed membranes were then separated into 1 ml aliquots, brought to 1% DDM, 1% TX-100 or 2% OG and rotated at 4 °C for 1 h. Following centrifugation at 114,000 × *g* for 30 min at 4 °C, supernatant fractions were incubated at room temperature for 10 h. The Soret band of Cyt *b* was measured at various time points and stability judged by the intensity of heme spectrum.

Protein stability was also assessed by monitoring the susceptibility of purified Cyt *b* to proteolytic degradation. Resistance to proteolytic degradation was followed by both quantitation of the heme Soret band and by SDS-PAGE analysis at various time points following incubation of Cyt *b* with V8 protease (15:1 Cyt *b*/V8 w/w) at 37 °C.

2.6. Determination of heme to protein ratio

Determination of the heme content of purified Cyt *b* was conducted by direct measurement of the Soret band using an extinction coefficient of 131,000 M^{-1} cm^{-1} for oxidized protein [14]. Alternatively, heme content was determined from reduced *minus* oxidized difference spectra for alkaline extracted pyridine hemochrome [15]. Briefly, oxidized spectra were collected following addition of 15 μl of pyridine and 7.5 μl of 1 N NaOH to 63 μl of purified Cyt *b*. Reduced spectra were obtained following addition of 1 μl of 1 M sodium dithionite and pyridine hemochrome content calculated from $\Delta\varepsilon_{559} = 20{,}700$ M^{-1} cm^{-1}.

Protein determination was conducted both by absorption spectroscopy and from densitometry of silver stained SDS-PAGE gels using BSA as a standard. Protein concentration from absorption measurements was conducted using an $\varepsilon_{280} = 143{,}240$ M^{-1} cm^{-1} calculated from the primary sequence of the Cyt *b* heterodimer using the program ProtParam at http://ca.expasy.org/tools/#primary. Protein purity (%Cyt *b*) of the various preparations was judged by densitometry of silver-stained gels to account for minor

contaminants and better assess the relative contribution of Cyt *b* to the measured protein absorption spectrum.

For densitometric analysis of protein concentration from silver-stained SDS-PAGE gels, various amounts of purified Cyt *b* were resolved and evaluated against known concentrations of BSA. Analysis was conducted such that the various loadings of BSA, gp91^{phox} and p22^{phox} fell in a linear range, with the parameters density/μg (BSA) and density/μl (gp91^{phox} and p22^{phox}) obtained from the slopes of each line.

2.7. MALDI mass spectrometry

For mass determination of p22^{phox}, Cyt *b* from peak gel filtration chromatography fractions was directly added to an equal volume of a saturated solution of α-cyano-4-hydroxycinnamic acid in 50% acetonitrile/0.3% TFA. This mixture (0.5 μl) was spotted and allowed to air dry on the MALDI plate. Mass spectra were obtained in the positive ion mode and were averaged over 128 laser shots. External mass calibration was performed by analysis of cytochrome *c* under identical conditions.

2.8. Functional reconstitution

Cyt *b* was relipidated following purification in DDM using SM-2 BioBeads as described below or was relipidated following elution from the affinity matrix in OG by previously described dialysis and dilution methods [16]. For reconstitution following purification in DDM, the SM-2 BioBeads used for detergent removal were washed three times in dH_2O and stored in dH_2O prior to use. Phosphatidylcholine was dissolved at 5 mg/ml in 50 mM NaH_2PO_4/1 mM EGTA/1 mM $MgCl_2$/20% glycerol/0.05 mM DTT, pH 7.4 (reconstitution buffer) with 1% DDM and lipids were dispersed by sonication. Following Cyt *b* purification, 40 μg of Cyt *b* was combined with 400 μg of lipid (~ 400 μl total sample volume) to obtain a 10:1 lipid to protein ratio (w/w). Samples were then dialyzed overnight at 4 °C against 1 l of reconstitution buffer for buffer exchange and removal of elution peptide. Reconstitution was achieved by rotating samples for 3–5 h at room temperature following addition of ~ 150 μl of packed SM-2 Biobeads. Control reconstitution reactions consisted of lipids alone treated in an identical fashion to form vesicles in the absence of Cyt *b*.

2.9. Cell-free NADPH oxidase assay

Neutrophil cytosol was prepared as described using LPS-free reagents [17]. A discontinuous 5–20% Percoll gradient was used to fractionate the subcellular constituents. Superoxide assays were performed in Costar 3370 96-well microtiter plates in an assay buffer consisting of the following final concentrations: 47 mM NaH_2PO_4, 18 mM K_2HPO_4, 1 mM $MgCl_2$, 1 mM EGTA, 2 mM NaN_3, 100 μM cytochrome *c*, 125 μM LDS, 10 μM FAD, 200 μM NADPH, 125 μM GTPγS, and 2×10^6 to 1×10^7 cell equivalents of the cytosol, in a total volume of 200 μl. All components of the cell-free assay except for NADPH were preincubated for ~ 5 min at room temperature, at which point superoxide production was initiated by the addition of NADPH. Superoxide was measured as the SOD-inhibitable reduction of cytochrome *c* and quantitated using $\Delta\varepsilon_{550} = 21{,}000\ M^{-1}\ cm^{-1}$ [18] blanked against identical wells containing 310 U/ml SOD. Average rates of superoxide generation were calculated from the linear region of increase in absorbance at 550 nm.

3. Results

3.1. Purification of Cyt b

Although purification schemes for human neutrophil Cyt *b* have been described [19,20], a substantially more rapid and efficient procedure was sought for isolation of this low abundance integral membrane protein. The Cyt *b* mAb 44.1 has been previously characterized [12] and maps to a surface accessible, discontinuous epitope on p22^{phox}. mAb 44.1 demonstrates a high affinity for Cyt *b* and its epitope-mimicking peptide (AC-PQVRPI-$CONH_2$) has been shown to potently dissociate complexes of the two proteins [12]. These properties suggested that a 44.1 protein A–Sepharose matrix, with peptide elution, could serve as an immunoaffinity purification system for isolation of Cyt *b* without exposure to denaturing conditions.

The purity of Cyt *b* after various stages of extraction of neutrophil plasma membranes with DDM and subsequent immunoaffinity purification is shown in Fig. 1. As demonstrated by SDS-PAGE analysis, DDM-solubilized Cyt *b* has been purified to near homogeneity following a single step consisting of adsorption and elution from the 44.1 affinity matrix (Fig. 1, lane 5). Affinity-purified Cyt *b* fractions contain high concentrations of the elution peptide (1 mM), which was removed by either dialysis or gel filtration chromatography. The efficiency of all steps was assessed by quantitation of the cytochrome Soret band (Table 1). These measurements indicate that approximately 46% of extracted protein was recovered from the affinity matrix, with approximately 85% of this eluted material recovered following concentration and an overnight dialysis step for removal of elution peptide.

Fig. 2 shows the purity of Cyt *b* at each step following extraction of intact neutrophils with DDM and subsequent purification by heparin and immunoaffinity chromatography. Similar to the situation when starting with neutrophil plasma membrane fractions, SDS-PAGE analysis (Fig. 2, lane 6) shows that Cyt *b* has been purified to near homogeneity when the highly contaminated, bulk heparin eluate is further purified on the 44.1 affinity matrix. Western blot analysis indicated the additional bands of ~ 25 and 50 kDa observed on the gel in Fig. 2 to be the heavy and light chains of mAb 44.1, which occasionally leaches from the affinity column in

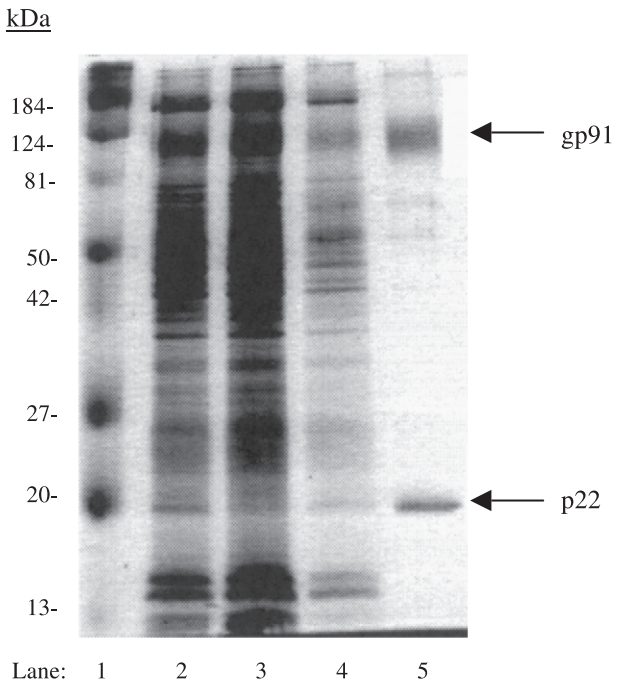

Fig. 1. Extraction and purification of Cyt *b* from neutrophil plasma membranes. Protein was evaluated by silver staining after separation on a 12% SDS-PAGE. Lane 1, molecular weight protein standards; lane 2, supernatant following solubilization of membranes with DDM; lane 3, material not adsorbed on the 44.1 affinity matrix; lane 4, material resulting from column wash steps; lane 5, 44.1 affinity matrix elution fractions.

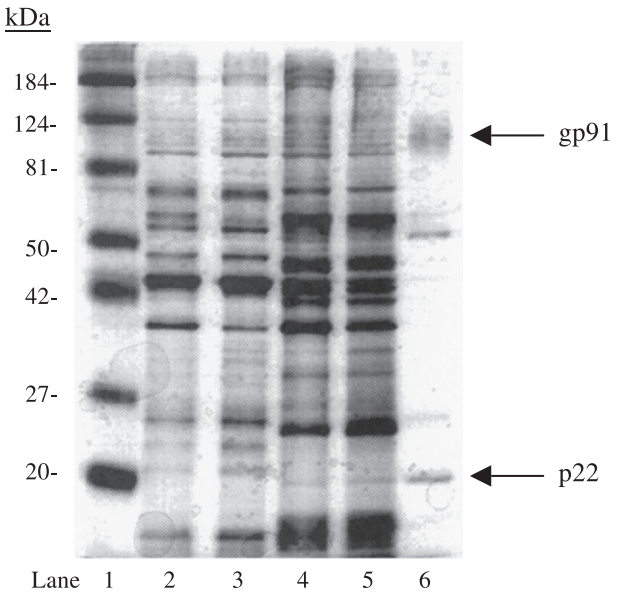

Fig. 2. Extraction and purification of Cyt *b* from intact neutrophils. Protein was evaluated by silver staining after separation on a 12% SDS-PAGE. Lane 1, molecular weight protein standards; lane 2, supernatant following solubilization of intact neutrophils with DDM; lane 3, material not adsorbed on heparin–agarose; lane 4, material eluted from heparin–agarose; lane 5, material not adsorbed to the 44.1 affinity matrix; lane 6, 44.1 affinity matrix elution fractions.

small amounts during purification. Whole-cell preparations starting with $\sim 4.5 \times 10^9$ intact neutrophils (equivalent to 10 ml of plasma membranes) typically yielded 75–100 μg Cyt *b* following affinity chromatography, resulting in roughly a 2-fold increase in protein compared to preparations starting with plasma membrane fractions.

3.2. Stability of detergent-solubilized Cyt b

To assess the stability of Cyt *b* in the presence of commonly employed nonionic detergents, the endogenous heme spectrum of the protein was monitored over time in neutrophil membrane extracts and during degradation of purified material by Staphylococcal V8 protease. The heme prosthetic groups reside close to or within the transmembrane region of Cyt *b* [9] and the heme spectrum provides a convenient measure of the structural integrity of the detergent-binding portion of the molecule. Fig. 3A shows the intensity of the Cyt *b* Soret band following extraction of neutrophil membranes with DDM, TX-100 or OG during incubation at room temperature over a 10-h time period. While roughly 70% of the heme spectrum remains intact for both DDM and Triton-solubilized protein, heme spectrum is rapidly lost following solubilization in OG with less that 30% of the original signal present after 10 h of incubation.

Spectral analysis of purified Cyt *b* following exposure to V8 protease indicated the persistence of a native-like heme spectrum after both 4.5 h (~ 64% of the original intensity, $\lambda_{max} = 413$ nm) and 11 h (~ 60% of the original intensity, $\lambda_{max} = 412$ nm) of proteolytic digestion (Fig. 3B). Maintenance of the native-like heme spectrum after prolonged digestion markedly contrasts similar studies recently conducted in TX-100 (see Fig. 2 in Ref. [9]), where a broadened and blue-shifted Soret peak (~ 60% of the original intensity, $\lambda_{max} = 409$ nm) was observed after only 4.5 h of exposure to V8 protease under similar conditions. While the heme spectrum became quite stable after 4.5 h for DDM-solubilized protein, the spectrum of TX-100 solubilized Cyt *b* continued to degrade, with little identifiable Soret absorbance remaining after 11 h of proteolytic digestion (T. Foubert, unpublished data). SDS-PAGE analysis of the various time points throughout the V8 digest of DDM-

Table 1
Immunoaffinity purification of human neutrophil Cyt *b*

Sample	Volume (ml)	Cyt *b* (pmol)	Recovery (%)
DDM extract	20	3094 ± 467 ($n = 6$)	100
44.1 affinity column	6	1420 ± 320 ($n = 6$)[a]	45.7 ± 6.3 ($n = 6$)[b]

Recoveries of Cyt *b* were determined for each step of the isolation procedure from neutrophil membranes (1×10^{10} cell equivalents) by measurement of the Soret band ($\varepsilon_{414} = 131{,}000\ M^{-1}\ cm^{-1}$).

[a] Yields from whole cell preparations were ~ 1000 pmol Cyt *b*/4.5×10^9 cells.

[b] Overall recoveries of ~ 40% are observed if protein is concentrated and dialyzed for peptide removal and ~ 33% if peptide is removed by gel filtration chromatography.

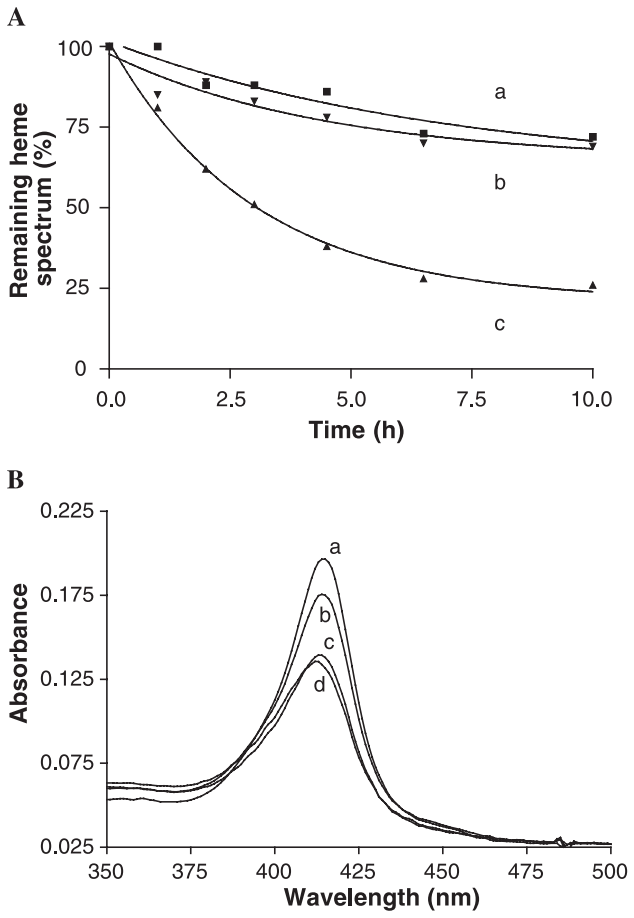

Fig. 3. Stability of Cyt *b* in DDM. (A) Following solubilization of neutrophil plasma membranes with 1% DDM (a), 1% TX-100 (b), or 2% OG (c); supernatant fractions were incubated for 10 h at room temperature. The intensity of the heme Soret band (414 nm) was evaluated at different time periods as a measure of Cyt *b* stability. (B) Resistance of purified Cyt *b* to proteolytic degradation was assessed by monitoring the heme Soret band at various time points following addition of V8 protease (15:1 Cyt *b*/V8 w/w) at 37 °C. Curve a, intact Cyt *b*; curve b, 1 h digest; curve c, 4.5 h digest; and curve d, 11 h digest. The retention of a native-like heme spectrum at 4.5 and 11 h contrasts results obtained with TX-100 solubilized Cyt *b* [9].

solubilized Cyt *b* confirms the accumulation of a recently characterized, stable ~60–66 kDa glycosylated fragment of gp91^{phox} and a stable ~17 kDa fragment of p22^{phox}, which are able to maintain the integrity of the heme spectrum [9] (R. Taylor, unpublished data). In contrast to the DDM studies, these stable digest fragments were gradually lost following only 1 h of V8 digestion for TX-100 solubilized protein [9], further demonstrating the enhanced stabilization of the transmembrane domain of Cyt *b* DDM.

3.3. Determination of heme stoichiometry

Although previous studies have suggested the presence of two heme prosthetic groups in the Cyt *b* heterodimer [5–8], a direct determination of heme content has yet to be reported. For direct determination of heme to protein stoichiometry, two distinct methods were employed to quantitate both heme (Soret band absorbance and pyridine extraction) and protein (absorption spectroscopy and densitometry) following affinity purification of Cyt *b*. Fig. 4A shows a representative absorption spectrum of affinity-purified Cyt *b* allowing for direct evaluation of both heme and protein content. To account for the contribution of minor contaminants that occurred to various degrees in the Cyt *b* purifications, densitometry was conducted on silver-stained SDS-PAGE gels for determination of the Cyt *b* component of the observed absorption spectrum. Quantitation of pyridine hemochrome (Fig. 4B) following pyridine extraction of samples was used to confirm estimates of heme content derived from direct evaluation of the Cyt *b* Soret band (Fig. 4A). Confirmation of protein concentrations determined from absorption spectra was obtained by densitometric analysis of silver-stained SDS-PAGE gels and comparison to known amounts of BSA electrophoresed on the same gel (data not shown). Averaging together all of the

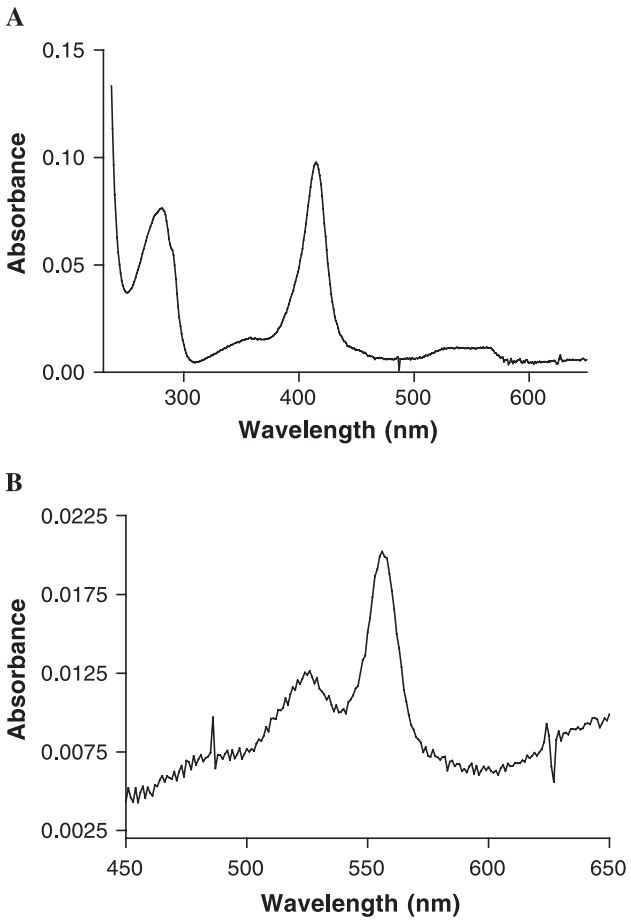

Fig. 4. Determination of the heme content of isolated Cyt *b*. (A) Absorption spectrum of purified Cyt *b* showing both the Soret band for oxidized heme and protein absorption from aromatic amino acids. Heme content was estimated based on an $\varepsilon_{414} = 131\ mM^{-1}\ cm^{-1}$ while protein concentration was determined using an $\varepsilon_{280} = 143.2\ mM^{-1}\ cm^{-1}$ calculated from primary sequence. (B) Heme quantitation from the reduced *minus* oxidized spectrum of pyridine hemochrome. Results obtained confirm the estimates of heme content based on the oxidized Soret band shown in A.

Table 2
Determination of the heme stoichiometry of Cyt *b*

Method for determination of heme/protein stoichiometry	Heme/protein stoichiometry	Overall heme/protein stoichiometry
Soret absorbance/OD_{280}	1.58 ± 0.13 (n = 5)	
Pyridine extraction/OD_{280}	1.88 ± 0.28 (n = 3)	1.80 ± 0.29 (n = 11)
Soret absorbance/ densitometry	2.15 (n = 1)	
Pyridine extraction/ densitometry	2.09 ± 0.22 (n = 2)	

Following immunoaffinity purification of Cyt *b*, relative concentrations of both protein and heme were determined as described in Materials and methods. Values obtained from the various methods indicated a 2:1 heme to protein stoichiometry for Cyt *b*.

data obtained from the above experiments indicated a heme/protein stoichiometry of 1.80 (± 0.30):1. Values obtained from the various methods of estimating heme to protein stoichiometry are shown in Table 2 and provide the first direct measurement of a 2:1 heme stoichiometry for Cyt *b*.

3.4. MALDI mass spectrometry

Following affinity purification and gel filtration chromatography, peak Cyt *b* elution fractions were combined with a equal volume of a saturated solution of α-cyano-4-hydroxycinnamic acid and analyzed by MALDI mass spectrometry. Fig. 5 shows the resulting spectra with peaks observed at 20,875.4 and 10,468.1 Da. Spectra are consistent with the observed ions as the singly and doubly protonated forms of $p22^{phox}$, which has a calculated molecular weight of 20,827.2 Da following proteolytic processing of the N-terminal methionine residue [9]. The observed spectra confidently identify $p22^{phox}$ with a mass accuracy of ~ 0.2%. Spectra for the $gp91^{phox}$ portion of the Cyt *b* heterodimer were not observed in the present study, most likely due to the relatively large molecular weight of this subunit and the extensive mass heterogeneity resulting from glycosylation.

3.5. Functional reconstitution

To measure the functional activity of Cyt *b* following purification in DDM, protein was incorporated into phosphatidylcholine vesicles previously shown to support NADPH oxidase activity. Since the critical micelle concentration (CMC) of dodeclymaltoside is too low for efficient reconstitution by dialysis or dilution methods, SM-2 Bio-Beads were employed for detergent removal and proteoliposome formation following affinity purification in this detergent. In a separate set of experiments, Cyt *b* was eluted from the affinity matrix in OG and reconstituted by previously described methods [16] for the purpose comparison to protein reconstituted using SM-2 BioBeads.

Fig. 6A shows a time course of SOD-inhibitable, cytochrome *c* reduction (a measure superoxide generation by NADPH oxidase) when reconstituted Cyt *b* was evaluated in a cell-free activity assay. Fig. 6B shows a smoothed absorbance spectrum indicating the Cyt *b* content of proteoliposomes used to generate the activity curve shown in Fig. 6A. Similar rates of superoxide production were observed for Cyt *b* either reconstituted following purification in DDM using SM-2 BioBeads or reconstituted following purification in OG using dialysis and dilution methods. Maximum rates of ~ 55 mol O_2^-/mol Cyt *b*/s were observed for reconstituted material in our cell-free assays and reconstituted protein consistently generated 2–3-fold higher rates

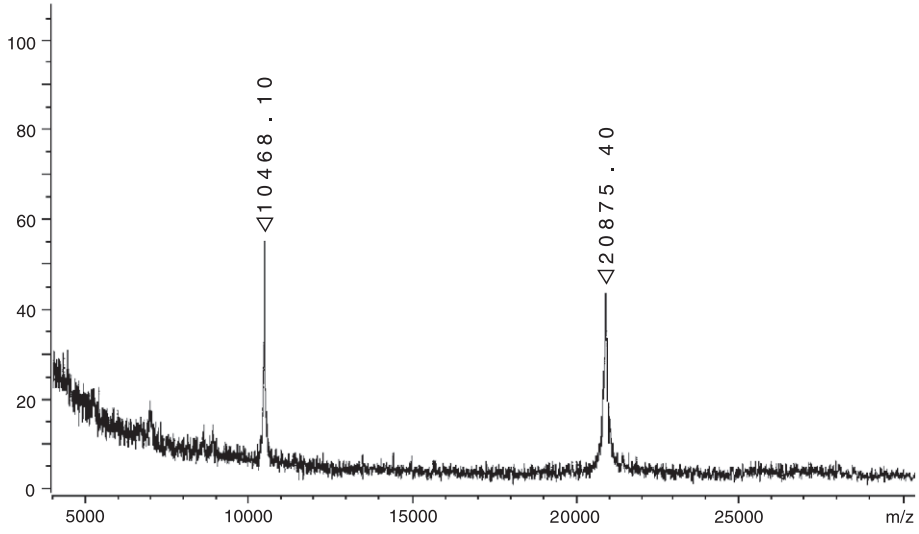

Fig. 5. MALDI analysis of Cyt *b* in the presence of the nonionic detergent DDM. Purified Cyt *b* fractions were added to an equal volume of a saturated solution of α-cyano-4-hydroxycinnamic acid and analyzed by MALDI mass spectrometry. Spectra obtained are consistent the singly (20,875.4 Da) and doubly protonated (10,468.1 Da) ions of $p22^{phox}$ and demonstrate a mass accuracy of ~ 0.2% relative to calculations based on gene sequence (20,827.2 Da for protein lacking the N-terminal methionine).

than observed for plasma membrane fractions used as starting material for purification. This observation demonstrates that the catalytic activity of Cyt *b* is effectively retained throughout the immunoaffinity purification procedure. Superoxide production by both membrane fractions and reconstituted Cyt *b* was observed to increase linearly with neutrophil cytosol, indicating that this reagent was not supplied at saturating levels in our cell-free assays.

3.6. Aggregation state

Since the nonionic detergent DDM has yet to be reported for purification of Cyt *b*, size exclusion chromatography was employed to ascertain the aggregation state of protein following purification. Fig. 7 shows a representative chromatogram monitoring the absorption of the Cyt *b* heme prosthetic groups when protein eluted from the immunoaffinity matrix is analyzed on a Superdex 200 gel filtration column. The retention time of the major peak on the gel filtration column (comprising ~85–90% of the total observed heme spectrum) indicated a molecular weight of approximately 350 kDa for the protein–detergent complex. These results are consistent with Cyt *b* that is purified as a monomeric species assuming that protein binds approximately an equal mass of detergent and displays an axial ratio of 6–8:1 [21,22]. These results are also in accordance with gel filtration data recently published by our group for TX-100 solubilized protein [9], previously shown to be monomeric by hydrodynamic analysis [22]. A preliminary assessment by dynamic light scattering demonstrated the affinity-purified Cyt *b* sample to show a monomodal distribution, consistent with a monodisperse protein–detergent complex (S. Ramaswami, unpublished data).

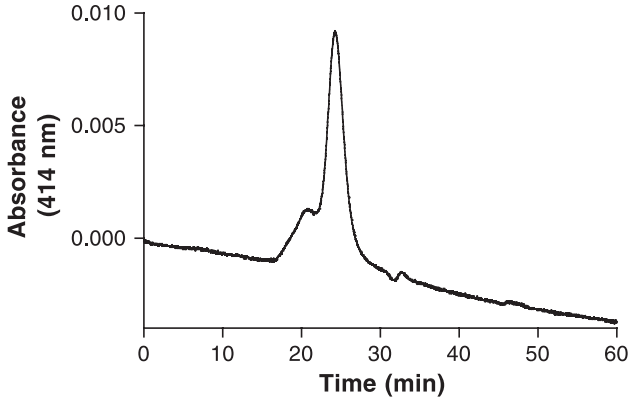

Fig. 7. Analysis of the molecular weight and aggregation state of Cyt *b* by size exclusion chromatography. Following purification by immunoaffinity chromatography, Cyt *b* was chromatographed on a calibrated Superdex-200 gel filtration column. The retention time and peak shape of the Cyt *b* chromatogram indicate that protein is isolated as a primarily monodisperse, protein–detergent complex of ~350 kDa.

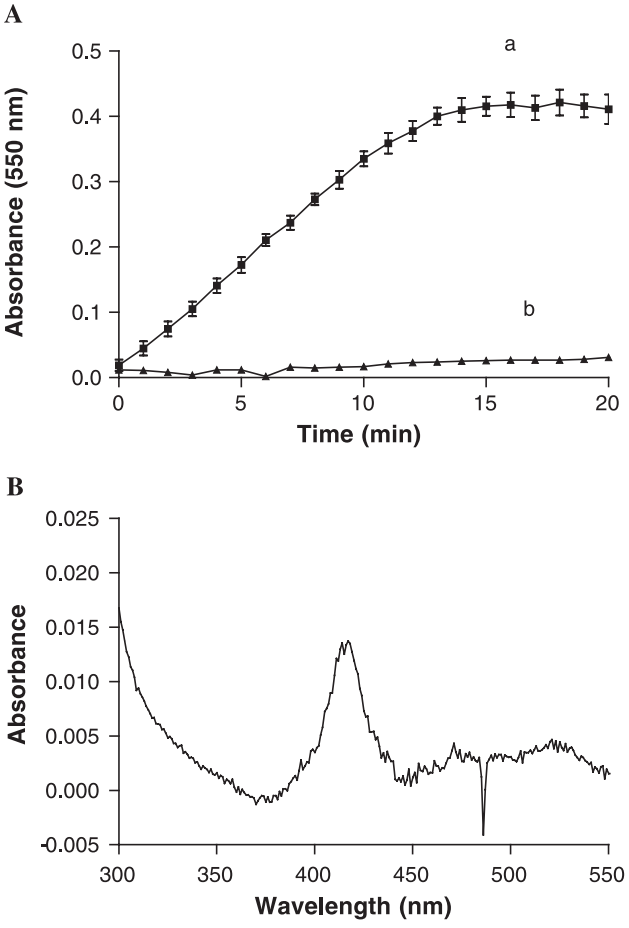

Fig. 6. Functional reconstitution of affinity purified Cyt *b*. (A) Following purification, Cyt *b* was mixed with DDM-solubilized lipids, detergent was removed by incubation with SM-2 BioBeads, and a cytochrome *c* reduction assay was used as a measure of electron transfer through Cyt *b*. Curve a, reconstituted Cyt *b*; curve b, lipid vesicles alone. (B) Smoothed absorption spectrum of reconstituted Cyt *b* for quantitation of the protein content of proteoliposomes used to generate the activity curve in A.

4. Discussion

4.1. Purification of Cyt b

Difficulties associated with obtaining adequate levels of purified protein have limited the amount of direct structural information reported for human neutrophil Cyt *b*. Due to its relatively high affinity for detergent-solubilized Cyt *b* and the ability of the peptide AC-PQVRPI-$CONH_2$ to effectively inhibit this interaction at submicromolar concentrations, the mAb 44.1 [12] was immobilized on protein A–Sepharose and tested for its properties as an affinity matrix. Following solubilization in DDM, Cyt *b* could be purified to near homogeneity in a single step from neutrophil plasma membrane extracts. The entire immunoaffinity procedure can be readily completed in a single day with nearly half of the initially extracted starting material recovered following elution from the affinity matrix. Reasonable efficiencies prove to be of critical importance in this situation as Cyt

b is a fairly low abundance integral membrane protein for which high-level expression systems are currently unavailable. The isolation of Cyt *b* following direct solubilization of intact neutrophils results in substantially increased levels of purified protein and also demonstrates the robust nature of the immunoaffinity purification method.

Several features of the purification procedure required optimization and are worthy of mention: (1) mAb 44.1 requires special handling as acid elution steps commonly employed for antibody elution following purification on protein A–Sepharose lead to both aggregation and loss of activity. The need to purify 44.1 was circumvented by directly loading crude hybridoma supernatant onto protein A–Sepharose beads for construction of the affinity matrix. Affinity columns constructed in this manner gave more consistent results and resulted in higher yields than columns constructed with 44.1 fractions that had been previously purified by a combination of ammonium sulfate fractionation and protein A–Sepharose. (2) The choice of detergent proved highly important for affinity purification of Cyt *b*. Aside from its ability to provide enhanced stability following solubilization, both binding to and elution from the 44.1 affinity matrix was notably more efficient in the detergent DDM compared to both TX-100 and OG. (3) For single step purification from membranes, solubilization at room temperature proved critical. When detergent extracts were prepared at 4 °C and then incubated with the 44.1 column at room temperature, solutions would develop a varying degree of turbidity (somewhat reminiscent of liposome formation) resulting in diminished recoveries of Cyt *b*. A heparin chromatography step prior to affinity purification eliminates such turbidity and should be included if initial solubilization at 4 °C is desired for purification from membrane fractions. (4) Although we have recently shown that several monoclonal antibodies recognizing the small subunit inhibit superoxide production in the cell-free assays, mAb 44.1 has no effect on the catalytic activity of Cyt *b* (J. Burritt, R. Taylor, A. Jesaitis, unpublished observations).

4.2. Stability of Cyt b

Integral membrane proteins can be quite unstable after being removed from their natural membrane environment [23]. Since solubilization is required for purification and biochemical characterization, it proves important to choose a solubilizing agent, that maintains the structural integrity of the individual protein under investigation. The nonionic detergent DDM has proven a popular choice for both purification and crystallization trials of integral membrane proteins due to its apparent ability to stabilize a wide array of integral membrane proteins following solubilization. Although TX-100 and OG have predominantly been employed for flavocytochrome purification [19,20], DDM proves an equally efficient solubilizer of neutrophil plasma membranes and appears to stabilize Cyt *b* to a greater extent. In addition to both protecting the protein against extensive degradation by V8 protease and better preserving the heme spectrum in neutrophil membrane extracts, DDM maintains the heme spectrum of purified Cyt *b* for well over a week at 4 °C (further time points have yet to be examined). The ability to preserve structural integrity over prolonged periods of time proves an essential characteristic of detergents employed for crystallization trials.

4.3. Heme stoichiometry of Cyt b

Previously proposed models suggesting the Cyt *b* heterodimer to contain two heme prosthetic groups have primarily based on: (1) potentiometric titration data measuring two distinct midpoint potentials, suggesting two distinct redox centers [6]; (2) EPR spectroscopy [7]; (3) comparison of primary sequence with other integral membrane cytochromes that employ a characteristic spacing of histidine residues on transmembrane α-helices for coordination of two heme ligands [5]; and (4) chemical modification studies showing two distinct reactivities of the Cyt *b* heme prosthetic groups to arylating agents [8]. Although good evidence exists for a two-heme Cyt *b* model, direct experimental determination of heme stoichiometry remained unreported. The purity and levels of protein obtained in the this study allowed for the first direct demonstration of a 2:1 heme/Cyt *b* stoichiometry.

Recent experimental evidence has confirmed long-standing models of Cyt *b* by identifying the proposed transmembrane regions as the heme bearing portion of the molecule [9]. Results from mutagenesis studies on Cyt *b* produced in a heterologous expression system have further suggested the heme coordinating histidine residues to reside in the transmembrane helices of the $gp91^{phox}$ subunit of the Cyt *b* heterodimer [24]. An alternative model proposes a situation in which one heme is coordinated by residues from $gp91^{phox}$ alone while the other coordinated by His94 of $p22^{phox}$ and a second histidine from one of the transmembrane helices of $gp91^{phox}$ [25]. Additional experimental evidence will be required to directly distinguish between the two proposed models and provide a more detailed structural view of the Cyt *b* heterodimer.

4.4. Mass analysis of $p22^{phox}$

Structure determination of integral membrane proteins is complicated by difficulties associated with overexpression, purification and production of crystals suitable for analysis by X-ray crystallography [23]. Although large, hydrophobic integral membrane proteins have proven challenging to analyze, mass spectrometry represents a particularly well-suited, alternative approach for obtaining direct structural information in difficult situations such as those presented by integral membrane proteins. MALDI studies on affinity-purified Cyt *b* demonstrate an accurate mass for $p22^{phox}$, as dictated by the gene sequence. This measurement represents

the first report of an accurate mass determination of this hydrophobic integral membrane protein by mass spectrometry. The MALDI data obtained is supported by both protein sequence data indicating the N-terminus of $p22^{phox}$ to begin at Gly2 as a results of proteolytic processing of the initiating methionine [9] and phage display studies localizing part of the discontinuous epitope of mAb 44.1 to the near extreme C-terminus of $p22^{phox}$ [12]. Although the analysis suggests that there has been no proteolytic degradation $p22^{phox}$ during the purification procedure, the observed average mass proves ~ 78 Da larger than predicted by gene sequence and cannot rule out the possibility of a post-translational modification. Previous studies have shown $p22^{phox}$ to be phosphorylated (an 80 Da modification) upon stimulation of neutrophils and activation of superoxide production [26]. It may be of interest that our membrane fractions are prepared from neutrophils that have been stimulated with fMLF in the presence of cytochalasin B.

The requirement for detergents to maintain the solubility of integral membrane proteins dictates the need to characterize detergents that are compatible with MALDI analysis as different detergents have been shown to either degrade or enhance ion formation [27]. Results obtained in this study suggest that the nonionic detergent DDM might prove valuable for mass determination of other integral membrane proteins.

4.5. Functional reconstitution of Cyt b

Although previous reconstitution protocols have employed either dialysis or dilution methods for reconstitution of Cyt *b* [16], the relatively low CMC of DDM precludes the use of either of these methods for incorporation of isolated protein into lipid vesicles. SM-2 BioBeads have a high capacity for the specific removal of detergents, regardless of the CMC, and have been demonstrated useful for both functional reconstitution and two-dimensional crystallization of integral membrane proteins [28]. Following removal of DDM with BioBeads and incorporation of Cyt *b* into phosphatidylcholine proteoliposomes, rates of superoxide generation were similar to rates observed with both Cyt *b* reconstituted from OG following affinity purification and starting membrane fractions used for Cyt *b* purification. Although active Cyt *b* has been generated by reconstitution with BioBeads, spectral measurements indicate the reconstitution process to be highly inefficient with only about 10% of the original starting spectral activity successfully incorporated into lipid vesicles. Detergent exchange into OG following immunoaffinity purification represents an attractive option for relipidation as Cyt *b* is recovered with high efficiency by both dialysis and dilution reconstitution methods. Efforts are underway to optimize the BioBead reconstitution procedure in order to make this method a more viable option for initiating two-dimensional crystallization trials for Cyt *b* following purification in DDM.

4.6. Aggregation state of DDM-solubilized Cyt b

Due to their tendency to aggregate following disruption of the natural membrane bilayer, it proves of particular importance to elucidate solubilization conditions that maintain a monodisperse state of the particular integral membrane protein under examination. Numerous gel filtration column runs of DDM-solubilized Cyt *b* demonstrate a highly monodisperse, heterodimeric protein–detergent complex. Moreover, the sedimentation rate and distribution of the DDM solubilized protein in DDM-containing sucrose gradients was observed to be very similar to that of TX-100 and OG-solubilized protein (D. Baniulis, A. Jesaitis, unpublished observations), supporting the notion that the DDM-solubilized Cyt *b* is a simple heterodimer. The small amounts of higher molecular weight Cyt *b* species observed in our preparations (Fig. 7) most likely represent a combination of Cyt *b* dimers and Cyt *b*–mAb complexes as substoichiometric amounts of mAb 44.1 (leached from the affinity matrix) are observed to co-purify in this minor gel filtration fraction. These small amounts of higher molecular weight Cyt *b* species are conveniently removed during gel filtration chromatography. The combination of purity, monodispersity and functional activity of Cyt *b* obtained in this study suggest the preparation suitable not only for biochemical studies, but also for two and three-dimensional crystallization trials necessary to facilitate the building of a more accurate structural model of Cyt *b*.

Acknowledgements

This work was supported by an Arthritis Foundation Postdoctoral Fellowship (to R.M.T.), American Heart Association SDG Award 30156N (to J.B.B.) and by the United States Public Health Service Grant R01 AI 26711 (to A.J.J.).

We would like to thank S. Ramaswami for conducting preliminary light scattering experiments on immunoaffinity-purified flavocytochrome *b*.

References

[1] J.T. Curnutte, M.C. Dinauer, in: G. Stamatoyannopoulis, et al. (Eds.), The Molecular Basis of Phagocyte Blood Diseases, Saunders, Philadelphia, 2001, pp. 539–563.
[2] R.M. Smith, J.T. Curnutte, Blood 77 (1991) 673–686.
[3] S.J. Weiss, N. Engl. J. Med. 320 (1989) 365–376.
[4] S.A. Weitzman, A.B. Weitberg, E.P. Clark, T.P. Stossel, Science 227 (1985) 1231–1233.
[5] C.A. Parkos, M.T. Quinn, S. Sheets, A.J. Jesaitis, in: A.J. Jesaitis, E.A. Dratz (Eds.), Molecular Basis of Oxidative Damage by Leukocytes, CRC Press, Boca Raton, FL, 1992, pp. 45–55.
[6] A.R. Cross, J. Rae, J.T. Curnutte, J. Biol. Chem. 270 (1995) 17075–17077.
[7] J.K. Hurst, T.M. Loehr, J.T. Curnutte, H. Rosen, J. Biol. Chem. 266 (1991) 1627–1634.
[8] J. Doussiere, J. Gaillard, P.V. Vignais, Biochemistry 38 (1999) 3694–3703.

[9] T.R. Foubert, J.B. Bleazard, J.B. Burritt, J.M. Gripentrog, D. Baniulis, R.M. Taylor, A.J. Jesaitis, J. Biol. Chem. 276 (2001) 38852–38861.
[10] W.R. Taylor, D.T. Jones, A.W. Segal, Protein Sci. 2 (1993) 1675–1685.
[11] V. Koshkin, E. Pick, FEBS Lett. 327 (1993) 57–62.
[12] J.B. Burritt, S.C. Busse, D. Gizachew, D.W. Siemsen, M.T. Quinn, C.W. Bond, E.A. Dratz, A.J. Jesaitis, J. Biol. Chem. 273 (1998) 24847–24852.
[13] C.A. Parkos, R.A. Allen, C.G. Cochrane, A.J. Jesaitis, J. Clin. Invest. 80 (1987) 732–742.
[14] R. Lutter, M.L.J. van Schaik, R. van Zwieten, R. Wever, D. Roos, M.N. Hamers, J. Biol. Chem. 260 (1985) 2237–2244.
[15] J.H. Fuhrhop, K.M. Smith, in: K.M. Smith (Ed.), Porphyrins and Metalloporphyrins, Elsevier, Amsterdam, 1975, pp. 804–807.
[16] S. Knoller, S. Shpungin, E. Pick, J. Biol. Chem. 266 (1991) 2795–2804.
[17] R.A. Clark, K.G. Leider, D.W. Pearson, W.M. Nauseef, J. Biol. Chem. 262 (1987) 4065–4074.
[18] V. Massey, Biochim. Biophys. Acta 34 (1959) 255–256.
[19] A.M. Harper, M.J. Dunne, A.W. Segal, Biochem. J. 219 (1984) 519–527.
[20] M.T. Quinn, C.A. Parkos, A.J. Jesaitis, Methods Enzymol. 255 (1995) 477–487.
[21] S. Maneti, I. Dunia, M. le Maire, E.L. Benedetti, FEBS Lett. 233 (1988) 148–152.
[22] C.A. Parkos, R.A. Allen, C.G. Cochrane, A.J. Jesaitis, Biochim. Biophys. Acta 932 (1988) 71–83.
[23] J.P. Rosenbusch, J. Struct. Biol. 136 (2001) 144–157.
[24] K.J. Biberstine-Kinkade, F.R. DeLeo, R.I. Epstein, B.A. LeRoy, W.M. Nauseef, M.C. Dinauer, J. Biol. Chem. 276 (2001) 31105–31112.
[25] M.T. Quinn, M.L. Mullen, A.J. Jesaitis, J. Biol. Chem. 267 (1992) 7303–7309.
[26] D.S. Regnier, D.G. Greene, S. Sergeant, A.J. Jesaitis, L.C. McPhail, J. Biol. Chem. 275 (2000) 28406–28412.
[27] K.O. Bornsen, Methods Mol. Biol. 146 (2000) 387–404.
[28] J.L. Riguad, D. Levy, G. Mosser, O. Lambert, Eur. Biophys. J. 27 (1998) 305–319.